Majorana Edge States in Atomic Wires Coupled by Pair Hopping

Christina V. Kraus,[1,2] Marcello Dalmonte,[1] Mikhail A. Baranov,[1,2,3] Andreas M. Läuchli,[2] and P. Zoller[1,2]

[1]*Institute for Quantum Optics and Quantum Information of the Austrian Academy of Sciences, A-6020 Innsbruck, Austria*

[2]*Institute for Theoretical Physics, Innsbruck University, A-6020 Innsbruck, Austria*

[3]*RRC Kurchatov Institute, Kurchatov Square 1, 123182 Moscow, Russia*

(Received 7 February 2013; published 23 October 2013)

We present evidence for Majorana edge states in a number conserving theory describing a system of spinless fermions on two wires that are coupled by pair hopping. Our analysis is based on a combination of a qualitative low energy approach and numerical techniques using the density matrix renormalization group. In addition, we discuss an experimental realization of pair-hopping interactions in cold atom gases confined in optical lattices.

DOI: 10.1103/PhysRevLett.111.173004 PACS numbers: 37.10.Jk, 05.10.Cc, 71.10.Pm

At present there is significant interest in identifying physical setups where Majorana fermions (MFs) [1] emerge as a collective phenomenon in many-body quantum systems [2]. The motivation behind this search is twofold. First, the existence of MFs is intimately linked to the concept of topological phases and their exploration. Second, MFs provide, due to their topological nature, a promising platform for topological quantum computing and quantum memory [3–5]. In a seminal paper Kitaev pointed out a route towards the realization of MFs in a simple many-body system [6]: A 1D wire of spinless fermions with a p-wave pairing can exhibit a topologically ordered phase with zero-energy Majorana edge states (MESs). The key ingredient here is the coupling of the wire to a superconducting reservoir in a grand canonical setting, which is induced in complex solid state structures via the so-called proximity effect. Building on this result, a remarkable theoretical and experimental effort has been devoted to the search of alternative settings supporting topological superconductivity in both 1D condensed matter [7–18] and cold atom systems [19–23].

In contrast, we propose and investigate in this Letter an alternative route to create MESs with cold atoms in optical lattices in the absence of any reservoir. This is motivated by a series of recent findings [24–26], pointing out the possibility of stabilizing topological phases supporting MESs in a purely number-conserving setting by mutually coupling 1D wires. We propose a scheme, based on a system of cold atoms in state-dependent optical lattices [27] combined with Raman assisted tunneling processes, which allows us to generate ladder Hubbard-type Hamiltonians with *interwire pair tunneling* and, at the same time, to suppress interwire single particle tunneling. The wires are then coupled in such a way that the number of particles in each of the wires is conserved *modulo* 2, thus realizing a $\mathbb{Z}_2$ *mutual* parity symmetry.

Below, we discuss first the implementation of the pair tunneling terms, which relies on the energetic protection of the parity symmetry. Then, we present a many-body study of a lattice Hamiltonian consisting of two wires coupled by pair tunneling by means of both analytical and density-matrix-renormalization group techniques [28,29]. We provide qualitative and quantitative evidence of the emergence of a topological phase supporting MESs, and discuss their robustness with respect to disorder and possible realistic imperfections.

Double wire system.—We consider the following Hamiltonian [see Fig. 1(a)]

$$H = -\sum_j [(t_a a_j^\dagger a_{j+1} + t_b b_j^\dagger b_{j+1}) + \text{H.c.}] + W\sum_j (a_j^\dagger a_{j+1}^\dagger b_j b_{j+1} + \text{H.c.}), \quad (1)$$

where a_j ($a_j^\dagger$), b_j ($b_j^\dagger$) are fermionic annihilation (creation) operators defined on two distinct wires a and b, respectively. The first line describes intrawire single-particle hopping with the corresponding amplitudes $t_{a,b}$ (in the following we consider $t_a = t_b = t$ as it does not affect the results), and the last term is the *interwire* pair hopping with the amplitude W. The choice of the Hamiltonian (1), motivated by previous considerations of the number-conserving settings [24], stems from global symmetries and corresponding conserved quantities: Besides the total number of particles, $N = N_a + N_b = \sum_j a_j^\dagger a_j + b_j^\dagger b_j$, associated with the $U(1)$ symmetry, there is another conserved charge—the parity P_1 of one of the wires [say, the wire a, $P_1 = p_a = (-1)^{N_a}$] associated with a $\mathbb{Z}_2$ symmetry [30]. The conservation is guaranteed by the last term in H allowing only hopping of particles between the wires in pairs, and is the key requirement to access a topological phase with Majorana fermions. We now first show how such dynamics can be generated with cold atoms in optical lattices, and then present a many-body study of Eq. (1) supporting the existence of MESs.

Pair hopping with cold atoms.—The basic idea behind an atomic implementation of pair tunneling terms is to introduce offsets in optical lattice potentials, which

suppress the single particle hopping by energy constraints, while an energy conserving pair hopping is allowed and mediated by interactions (for an alternative implementation see [31]). An atomic setup illustrating these ideas is given in Figs. 2(a)–2(d). We implement the two wires of spinless fermions as a bipartite lattice for spinfull fermions [32,33]. A typical lattice scheme is illustrated in Figs. 1(b) and 1(c) for ^{40}K atoms, where the two spin states are encoded in the atomic states $|F = 9/2,\ m_F = 9/2\rangle$ and $|7/2,\ 7/2\rangle$; combining laser beams with different polarizations, a lattice of arrays of plaquettes in the xy plane is realized (see [34] for details on the laser scheme). Odd (even) and even (odd) lattice sites j on the upper (lower) wire trap the spin $\uparrow$ and $\downarrow$ components of the fermions, and transitions between adjacent wells (and the associated spin flip) are induced either by an rf field or by an optical Raman transition with Rabi frequency Ω and ω the optical frequency [35] [see Fig. 2(b)]. The spins are placed in a spatially varying magnetic field with the gradient perpendicular to the wires. Supplemented with a spin-independent lattice along the y axes, this results in a spin dependent energy offset [34]: the spins $\uparrow$ and $\downarrow$ on the (upper) a wire have energies ϵ_2 and $-\epsilon_1$, and the corresponding energies on the (lower) wire b are $-\epsilon_1$ and ϵ_2, respectively. If we choose $\omega = \epsilon_1 + \epsilon_2$, our model reduces again to a 1D tight binding model for spinless fermions hopping on the wires.

To understand the pair hopping mechanism, consider the plaquette indicated in Fig. 2(a) by the dashed line. We assume an auxiliary molecular site in the center of the plaquette (indicated as (C) in Fig. 2(a), which traps both $\uparrow$ and $\downarrow$ atoms, and is connected to the lattice sites on the wire by a spin-preserving tunneling coupling with amplitudes t_{am} and t_{bm}. Pairs of atoms occupying the molecular site are assumed to interact via an onsite interaction U, i.e.,

$$H_{0c} = \sum_{c\equiv(j,j+1)} U a^\dagger_{\uparrow c} a^\dagger_{\downarrow c} a_{\downarrow c} a_{\uparrow c} - \sum_{c\equiv(j,j+1)} \sum_{\alpha=a,b} t_{m\alpha}(a^\dagger_{\uparrow c} a_{j\uparrow,\alpha} + a^\dagger_{\downarrow c} a_{j+1\downarrow,\alpha} + \text{H.c.})$$

where we adopt the notation $c \equiv (j, j+1)$ for c on the link $j, j+1$. In addition, rf or Raman induced spin-flip transitions are generated in this setup. However, they are off-resonant and average to zero, so that they can be neglected in the following [34]. We can now write the corresponding Hamiltonian in a frame rotating with ω as

$$\begin{aligned}\tilde{H}_\square = {} & \epsilon_2 a^\dagger_{1a} a_{1,a} - \epsilon_1 a^\dagger_{2a} a_{2,a} - (\Omega a^\dagger_{1a} a_{2a} e^{-i2\epsilon t} + \text{H.c.}) \\ & + \epsilon_2 a^\dagger_{1b} a_{1,b} - \epsilon_1 a^\dagger_{2b} a_{2b} \\ & - (\Omega a^\dagger_{1b} a_{2b} e^{-i2\epsilon t} + \text{H.c.})(-\epsilon') \sum_{\sigma=\uparrow,\downarrow} a^\dagger_{\sigma c} a_{\sigma c} \\ & + U a^\dagger_{\uparrow c} a^\dagger_{\downarrow c} a_{\downarrow c} a_{\uparrow c} - t_{ma}[a^\dagger_{\uparrow c}(a_{1a} + a_{2b}) \\ & + a^\dagger_{\downarrow c}(a_{1b} + a_{2a}) + \text{H.c.}]. \end{aligned} \quad (2)$$

For the sites on the two wires we have used the notation $a_{1\uparrow,a} \to a_{1a}$, $a_{1\downarrow,b} \to a_{1b}$ and $a_{2\downarrow,a} \to a_{2a}$, $a_{2\uparrow,b} \to a_{2b}$. The first two lines are the Raman or rf hopping between sites

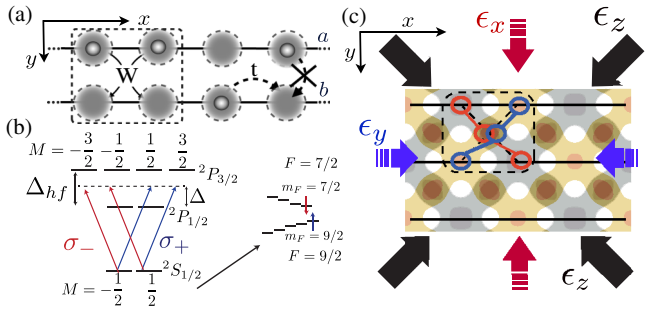

FIG. 1 (color online). (a) Ladder Hamiltonian: Atoms in the ground states a and b confined in the upper resp. lower wire can tunnel individually along the x direction, and can hop in pairs between the wires. (b) Atomic scheme for ^{40}K atoms: the two states $|F = 9/2,\ m_F = 9/2\rangle$ and $|7/2,\ 7/2\rangle$ serve as $\uparrow$ and $\downarrow$ spin states in the microscopic implementation, while laser beams of different polarizations realize the spin dependent potential (see [34]). (c) Typical lattice structure which realizes arrays of two-leg ladders: the circled areas correspond to the plaquette in panel (a). Black arrows denote counterpropagating beams on the xy plane with ϵ_z polarization, while red (blue) arrows describe counterpropagating beams in the $yz(xz)$ plane with $\epsilon_x(\epsilon_y)$ polarization with a $\pi/4$ angle with respect to $yz(xz)$.

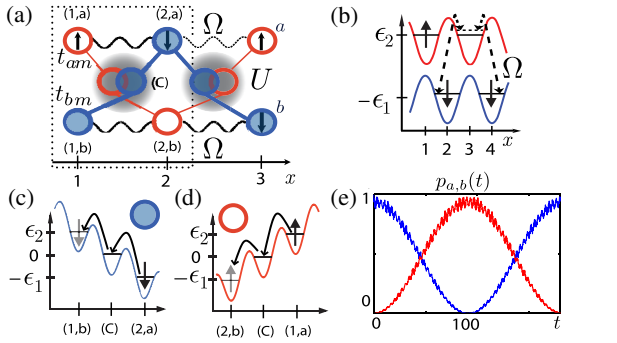

FIG. 2 (color online). (a)–(d): Implementation of the pair hopping: (a) Ladder setup as a combination of two wires with opposite energy offsets (b). The dashed box denotes a single plaquette, with site indices in parenthesis $(\cdots)$; t_{am}, t_{bm} are the tunneling amplitudes from the a and b wire to the central sites, respectively. Atoms in the center [(C)] of the plaquette interact with strength U (shaded area). (b) The single wire is realized as a bipartite lattice of $\uparrow$ and $\downarrow$ fermions with Raman-assisted tunneling (Rabi frequency Ω). (c),(d) Energy offsets along the diagonal of the plaquette in (c) for the $\downarrow$ resp, *d)* $\uparrow$ species, and corresponding virtual processes indicating pair tunneling (see text). The energy offsets $-\epsilon_1$ and ϵ_2 inhibit single particle hopping between the wires, while the pair hopping respects energy conservation. (e) Time evolution of the state $a^\dagger_{1,a\uparrow} a^\dagger_{2,a\downarrow}|0\rangle$ according to the microscopic dynamics of $\tilde{H}_\square$ (see text): the blue (red) curve indicate the population $p_{a,b}(t) = \langle n_{a/b,1} n_{a/b,2}\rangle$ as a function of time.

$2 \leftrightarrow 1$ with energies $-\epsilon_1$ and $+\epsilon_2$, respectively, due to absorption (emission) of a photon $\omega = \epsilon_1 + \epsilon_2$, which is tuned to compensate the energy difference. The third line corresponds to the central site with interaction and hopping. The last line then describes tunneling from the wires to the central site.

Let us now analyze the various processes on the plaquette according to the Hamiltonian (2). First, single particle hopping between the wires is suppressed: consider an atom, say in the upper wire a in lattice site 1 with spin $\uparrow$. Spin-preserving tunneling is possible via the molecular site along the diagonal of the plaquette (virtual processes are indicated in Figs. 2(c) and 2(d)). It corresponds to the process $\uparrow_{1a} \rightarrow \uparrow_m \rightarrow \uparrow_{2b}$, which is suppressed by the corresponding energy offsets $+\epsilon_2$, 0, $-\epsilon_1$. In a similar way, the tunneling of the $\downarrow$ atom along $\downarrow_{2a} \rightarrow \downarrow_m \rightarrow \downarrow_{1b}$ is also suppressed by energy conservation. For pair hopping $\uparrow_{1a}\downarrow_{2a} \rightarrow \uparrow\downarrow_m \rightarrow \uparrow_{2b}\downarrow_{1b}$, however, the overall energy will be conserved, since the two atoms can exchange energy via the interaction U. After adiabatic elimination of the intermediate sites when U, $\epsilon_{1/2} \gg t_{am,bm}$, the resulting amplitude for the pair-hopping term is [34]

$$W = -\left(\frac{1}{\epsilon_2} - \frac{1}{\epsilon_1}\right)^2 \frac{t_{am}^2 t_{bm}^2}{U}. \tag{3}$$

In Fig. 2(e) we present a numerical analysis of the pair-hopping dynamics of the state $a^\dagger_{1,a\uparrow} a^\dagger_{2,a\downarrow}|0\rangle$ subject to the Hamiltonian $\tilde{H}_\square$. Here, (in units of t_{am}) $t_{bm} = 1$, $\epsilon_2 = 2\epsilon_1 = 2$, $U = -20$. As we discuss in [34], the pair hopping term will generate further processes which can be suppressed by tilting the plaquette. Finally, in fourth order perturbation theory density-density interactions between particles on one plaquette emerge. They are induced by virtual processes where two particles from the site j, j' belonging to the same plaquette hop into the intermediate sites, and subsequently hop back to j, j'. The corresponding terms read $H_{\text{diag}} = K\sum_{j,j'}\sum_{\sigma,\sigma'=\uparrow,\downarrow}\sum_{\alpha,\alpha'=a,b} n_{j\sigma,\alpha} n_{j'\sigma',\alpha'}$, where K is of the same order as W. Note that these perturbations are also parity preserving. Further, as we show in [34], these terms only have a quantitative effect on the Majorana physics.

Majorana edge states in coupled wires.—The presence of a parity symmetry in Eq. (1) is at the heart of possible topological phases. We have investigated the phase diagram of H by means of both low-energy field theory based on bosonization, and mean field arguments: both approaches provide evidence of a superconducting phase supporting MES (a detailed analysis is provided [34]). We present here a numerical study by means of density-matrix-renormalization group simulations. We start with a brief description of the phase diagram of the system, and then identify the topological phase supporting the MES according to the following criteria: (i) two degenerate ground states with different parities for the individual wires in the case of open boundary conditions (OBCs), (ii) nonlocal fermionic correlations between the edges, coming along with (iii) topological order indicated by a degenerate entanglement spectrum, and (iv) robustness of the above properties against static disorder. In the following, we set $t = 1$ as the energy scale.

The phase diagram of the model can be divided into three regions: a superconducting phase, an insulating phase, and a region of phase separation. The superconducting phase is characterized by a homogeneous density, leading superconducting correlations, and nonzero single-particle gap $\Delta = |E_0(N) - \frac{1}{2}[E_0(N+1) + E_0(N-1)]|$ for periodic boundary conditions (PBCs). Here $E_0(N)$ is the ground state energy for N particles. We find this phase for small and moderate values of the pair hopping $|W| \lesssim 1$ and all fillings except $n = 1/2$. At exactly half-filling, an incompressible insulating phase is formed with exponentially decaying superconducting correlations. For large values of the pair hopping $|W| \gg 1$ we find phase separation with the formation of particle clusters. In the following we concentrate on the superconducting phase and check the criteria (i)–(iv). For our numerical analysis, we take $W = -1.8$ and the filling $n = 1/3$ as representative values resulting in a homogeneous superconducting phase for system sizes $L = 12$, 24 and $L = 36$ with even number of particles.

(i) The ground state degeneracy can be studied by looking at the energy gap $\Delta E_n(N) = E_n(N) - E_0(N)$ between the ground state and the nth excited state. As shown in Fig. 3(a), in the case of OBCs, the gap between the ground and the first excited state $\Delta E_{1,\text{OBC}}$ closes exponentially in

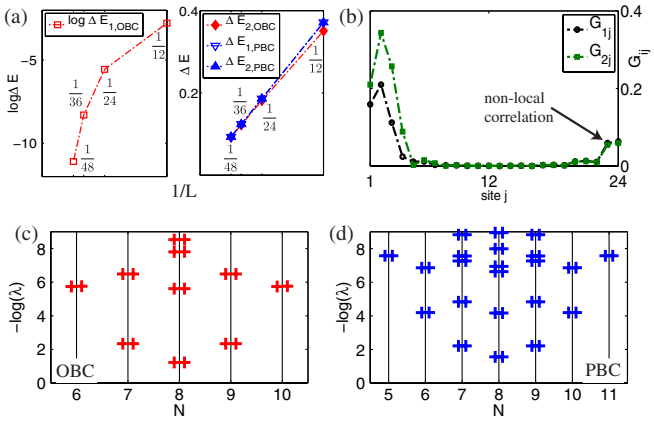

FIG. 3 (color online). (a) Closing of the energy gaps with the system size ($L = 12$, 24, 36) for $W = -1.8$ and $n = 1/3$. For OBCs, the gap ΔE_1 closes exponentially (left panel), in contrast to the polynomial closing in the case of PBCs (right panel, open blue triangles). The energy gap ΔE_2 closes polynomially independent of the boundary conditions (right panel, red diamonds for the OBC and closed triangles for PBC). Note that $\Delta E_{2,\text{PBC}} = \Delta E_{1,\text{PBC}}$. (b) Nonlocal fermionic correlations G_{lj} on the upper wire for $L = 24$. (c) and (d) Entanglement spectrum for the system of the size $L = 24$ shows double degeneracy for both the OBC (c) and PBC (d).

the system size (left panel) indicating the degeneracy of the ground state in the thermodynamic limit. This is in contrast to the case of the PBC that is depicted in the right panel of Fig. 3(a) (blue open triangles). Here we find that $\Delta E_{1,\mathrm{PBC}}$ closes linearly in the system size, and $\Delta E_{1,\mathrm{PBC}} = \Delta E_{2,\mathrm{PBC}}$; i.e., the first and second excited state are degenerate (blue open and closed triangles). For the OBC, $\Delta E_{2,\mathrm{OBC}}$ also closes linearly in the system size (red diamonds). We find that the two degenerate ground states in the case of OBCs differ by the parities of the individual wires. Note that for the OBC we also have $\Delta = 0$.

(ii) The intrawire single-particle correlation function $G_{lj} = \langle a_l^\dagger a_j \rangle$ for the system of the length $L = 24$ is shown in Fig. 3(b) for the case where $l = 1, 2$ is close to the left edge and $j \in [l, L]$. We see that G_{lj}, being exponentially small inside the wire, attains a finite value at the right edge showing the existence of nonlocal fermionic correlations typical for a system with MF edge states.

(iii) Topological order (TO) manifests itself in the degeneracy of the entanglement spectrum (ES) [36–38]: Let $\rho_A = \sum_{Nj} \lambda_j^{(N)} \rho_j^{(N)}$ be the reduced density matrix of the system with respect to some bipartition with support on both wires, where $\rho_j^{(N)}$ describes a pure state of N particles with the corresponding eigenvalues $\lambda_j^{(N)}$. In a topological phase, the low-lying eigenvalues $\lambda_j^{(N)}$ are expected to be doubly degenerate for each N, for both open and periodic boundary conditions, as it is demonstrated in Fig. 3(c) (OBC) and Fig. 3(d) (PBC) for a system of the size $L = 24$. Moreover, the distributions of the low-lying eigenvalues as a function of N share the same patter in the two cases. We have also verified that in the case of hard-core bosonic ladders with pair hopping, the ES does not show such structure, underlining the key role of Fermi statistics in determining topological features of the paired phase.

(iv) The robustness of the above properties against static disorder is one of the key manifestations of a nonlocal topological order. We model the disorder by adding the term $H_{V_r} = \sum_j V_j^{(a)} a_j^\dagger a_j + V_j^{(b)} b_j^\dagger b_j$ to the Hamiltonian, where $V_j^{(\gamma)}$with $\gamma = a, b$ are random local potentials equally distributed in the interval $[-V_r, V_r]$. We find that even for moderate disorder $V_r = 0.1t$, the ground state remains doubly degenerate, and the system still exhibits the nonlocal correlations [Fig. 4(a)] as well as the degenerate ES [Fig. 4(b)], indicating the presence of the topological order. For strong local disorder, however, the topological effects disappear, as we checked, e.g., for a value of $V_r = 1.5t$. In addition, we have investigated the effect of disorder in the pair hopping, which we model by an additional term $H_{W_r} = \sum_j W_j^{(a)} a_j^\dagger a_{j+1}^\dagger b_{j+1} b_j + \mathrm{H.c.}$, where we have taken W_j to be equally distributed within the interval $[-W_r, W_r]$. We find that even for $W_r = 0.1W$ the topological properties of the system survive. As an example, we present Fig. 4(c), the ES which maintains its doubly degenerate structure.

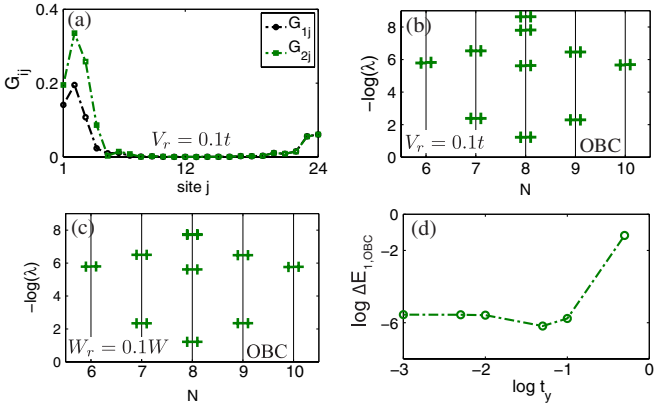

FIG. 4 (color online). Effects of imperfections on the topological order ($L = 24$, $n = 1/3$, OBC). (a),(b) Effects of static disorder: The nonlocal correlations (a) and the degeneracy of the ES (b) indicated the topological state in the presence of disorder with $V_r = 0.1t$. (c) Effect of disorder in the pair hopping. The ES remains degenerate. (d) Ground state degeneracy in the presence of an interwire single-particle hopping $H_\perp = \sum_i t_y a_i^\dagger b_i + \mathrm{H.c.}$

Remarkably, the observed topological order and its consequences are also stable against a single-particle hopping $H_\perp = \sum_i t_y a_i^\dagger b_i + \mathrm{H.c.}$ between the two wires, which breaks the parity of the wires and related Z_2 symmetry. As an example, we show in Fig. 4(d) the energy gap $\Delta E_{1,\mathrm{OBC}}$ as a function of t_y: The ground state of the system remains degenerate up to values t_y of the order of $0.1t$ [Fig. 4(d)], in agreement with the prediction of Refs. [24,25]. Note, however, that the dependence of $\Delta E_{1,\mathrm{OBC}}$ on L changes from exponential to power law [26]. This stability could be very important for experimental realizations of the model because the interwire single-particle hopping is one of the most probable imperfections.

Detection.—The emerging Majorana states can be detected following the proposals of Ref. [39], e.g., by using standard quantum optics detection tools like time-of-flight imaging and the spectroscopic technique to probe the ground state degeneracy and the inherent nonlocal fermionic correlations. Demonstration of a non-Abelian statistic of the MFs, on the other hand, requires some dynamical protocols resulting in the motion of MFs around each other. In our setup, one could think of a generalization of the ideas of Ref. [40] relying on single-site addressing available in current experiments with ultracold atoms [41,42]. Another possibility would be an atomic analog of the fractional Josephson effect [17] using a properly shaped external potential along the x direction.

Conclusions and outlook.—In summary, we have shown how topological states of matter with Majorana fermion edge states can be created in fermionic atomic ladders via a pair-hopping Hamiltonian without any additional reservoir or p-wave interaction. The proposed implementation of the

pair-hopping interaction in a cold atom system can also be used for the simulation of Abelian [43] and non-Abelian lattice gauge theories [44]. Further, one might also think to use it for the construction of an entangling quantum gate, where the hopping of one particle (control) triggers the tunneling of a second atom (target).

We thank N. Ali-Bray, M. Burrello, S. Manmana, J. D. Sau, F. Schreck, and H.-H. Tu for fruitful and useful discussions. M. D. acknowledges support by the European Commission via the integrated project AQUTE. We further acknowledge support by the Austrian Science Fund FWF (SFB FOQUS F4015-N16) and the Austrian Ministry of Science BMWF as part of the UniInfrastrukturprogramm of the Research Platform Scientific Computing at the University of Innsbruck.

[1] E. Majorana, Nuovo Cimento **14**, 171 (1937).
[2] F. Wilczek, Nat. Phys. **5**, 614 (2009).
[3] C. Nayak, S. H. Simon, A. Stern, M. Freedman, and S. D. Sarma, Rev. Mod. Phys. **80**, 1083 (2008).
[4] J. Alicea, Rep. Prog. Phys. **75**, 076501 (2012).
[5] C. W. J. Beenakker, Annu. Rev. Condens. Matter Phys. **4**, 113 (2013).
[6] A. Y. Kitaev, Phys. Usp. **44**, 131 (2001).
[7] J. D. Sau, R. M. Lutchyn, S. Tewari, and S. D. Sarma, Phys. Rev. Lett. **104**, 040502 (2010).
[8] R. M. Lutchyn, J. D. Sau, and S. D. Sarma, Phys. Rev. Lett. **105**, 077001 (2010).
[9] Y. Oreg, G. Refael, and F. von Oppen, Phys. Rev. Lett. **105**, 177002 (2010).
[10] M. Sato, Y. Takahashi, and S. Fujimoto, Phys. Rev. Lett. **103**, 020401 (2009).
[11] A. M. Tsvelik, arXiv:1106.2996.
[12] E. M. Stoudenmire, J. Alicea, O. A. Starykh, and M. P. A. Fisher, Phys. Rev. B **84**, 014503 (2011).
[13] M. Tezuka and N. Kawakami, Phys. Rev. B **85**, 140508(R) (2012).
[14] V. Mourik, K. Zou, S. M. Frolov, S. R. Plissard, E. P. A. M. Bakkers, and L. P. Kouwenhoven, Science **336**, 1003 (2012).
[15] M. T. Deng, C. L. Yu, G. Y. Huang, M. Larsson, P. Caroff, and H. Q. Xu, Nano Lett. **12**, 6414 (2012).
[16] A. Das, Y. Ronen, Y. Most, Y. Oreg, M. Heiblum, and H. Shtrikman, Nat. Phys. **8**, 887 (2012).
[17] L. P. Rokhinson, X. Liu, and J. K. Furdyna, Nat. Phys. **8**, 795 (2012).
[18] M. Sato and S. Fujimioto, Phys. Rev. B **79**, 094504 (2009).
[19] L. Jiang, T. Kitagawa, J. Alicea, A. R. Akhmerov, D. Pekker, G. Refael, J. I. Cirac, E. Demler, M. D. Lukin, and P. Zoller, Phys. Rev. Lett. **106**, 220402 (2011).
[20] S. Diehl, E. Rico, M. A. Baranov, and P. Zoller, Nat. Phys. **7**, 971 (2011).
[21] S. Nascimbène, J. Phys. B **46**, 134005 (2013).
[22] M. Sato, Y. Takahashi, and S. Fujimoto, Phys. Rev. Lett. **103**, 020401 (2009).
[23] M. Sato, Y. Takahashi, and S. Fujimoto, Phys. Rev. B **82**, 134521 (2010).
[24] M. Cheng and H.-H. Tu, Phys. Rev. B **84**, 094503 (2011).
[25] L. Fidkowski, R. M. Lutchyn, C. Nayak, and M. P. A. Fisher, Phys. Rev. B **84**, 195436 (2011).
[26] J. D. Sau, B. I. Halperin, K. Flensberg, and S. D. Sarma, Phys. Rev. B **84**, 144509 (2011).
[27] I. Bloch, J. Dalibard, and W. Zwerger, Rev. Mod. Phys. **80**, 885 (2008).
[28] S. R. White, Phys. Rev. Lett. **69**, 2863 (1992).
[29] U. Schollwöck, Rev. Mod. Phys. **77**, 259 (2005).
[30] The parity P_1 is equal to $(-1)^{(N_a-N_b)/2}$ up to a constant depending on N, and, therefore, the parity P_1 characterizes the antisymmetric sector of the theory.
[31] M. Dalmonte *et al.* (to be published).
[32] A. J. Daley, M. M. Boyd, J. Ye, and P. Zoller, Phys. Rev. Lett. **101**, 170504 (2008).
[33] F. Gerbier and J. Dalibard, New J. Phys. **12**, 033007 (2010).
[34] See Supplemental Material at http://link.aps.org/supplemental/10.1103/PhysRevLett.111.173004 for the realization of the spin-dependent lattice and the derivation of the pair hopping Hamiltonian.
[35] D. Jaksch and P. Zoller, New J. Phys. **5**, 56 (2003).
[36] F. Pollmann, A. M. Turner, E. Berg, and M. Oshikawa, Phys. Rev. B **81**, 064439 (2010).
[37] A. M. Turner, F. Pollmann, and E. Berg, Phys. Rev. B **83**, 075102 (2011).
[38] L. Fidkowski and A. Kitaev, Phys. Rev. B **83**, 075103 (2011).
[39] C. V. Kraus, S. Diehl, P. Zoller, and M. A. Baranov, New J. Phys. **14**, 113036 (2012).
[40] C. V. Kraus, P. Zoller, and M. A. Baranov, arXiv:1302.1824 [Phys. Rev. Lett. (to be published)].
[41] W. S. Bakr, J. I. Gillen, A. Peng, S. Fölling, and M. Greiner, Nature (London) **462**, 74 (2009).
[42] J. F. Sherson, C. Weitenberg, M. Endres, M. Cheneau, I. Bloch, and S. Kuhr, Nature (London) **467**, 68 (2010).
[43] H. P. Büchler, M. Hermele, S. D. Huber, M. P. A. Fisher, and P. Zoller, Phys. Rev. Lett. **95**, 040402 (2005).
[44] D. Banerjee, M. Bögli, M. Dalmonte, E. Rico, P. Stebler, U.-J. Wiese, and P. Zoller, Phys. Rev. Lett. **110**, 125303 (2013).